See next page.

REMOTE SENSING OF SURFACE EMISSIVITY WITH THE TELOPS HYPER-CAM

Steven Adler-Golden and Patrick Conforti
Spectral Sciences, Inc., Burlington, MA 01803

Marc-André Gagnon, Pierre Tremblay and Martin Chamberland
Telops Inc., Québec, Qc, Canada G2E 6J5

ABSTRACT

Processing long-wave infrared (LWIR) hyperspectral imagery to surface spectral emissivity or reflectance units via atmospheric compensation and temperature-emissivity separation (TES) affords the opportunity to remotely classify and identify surface materials with minimal interference from atmospheric effects. This paper describes an automated atmospheric compensation and TES method, called FLAASH-IR (Fast Line-of-sight Atmospheric Analysis of Spectral Hypercubes – Infrared), and its application to airborne imagery taken with the Telops Inc. Hyper-Cam interferometric hyperspectral imager. The results demonstrate good suppression of the atmospheric features due to water vapor and ozone, resulting in quantitative surface spectra, even with highly reflective (low emissivity) objects such as bare metal.

Index Terms— hyperspectral, thermal, infrared, emissivity, atmospheric correction

1. INTRODUCTION

Hyperspectral imaging (HSI) technology provides a wealth of information for remotely identifying and characterizing surface materials and objects based on their spectral signatures. Long-wave and mid-wave infrared (L/MWIR) HSI sensors yield both surface emissivity spectra and temperatures if the atmospheric effects are removed and the retrieved surface emission is factored into emissivity and Planck function components. Since precise knowledge of the atmospheric conditions is not generally available, the atmospheric description must be retrieved from the image itself. Removal of the atmospheric components is commonly called atmospheric compensation or correction, while the emissivity retrieval is called temperature/emissivity separation (TES).

Atmospheric compensation methods are less well established in the L/MWIR than in the visible-shortwave IR region due to the added complexity introduced by thermal emission. In addition, atmospheric compensation is formally an underdetermined problem: the atmospheric properties are usually imprecisely known, and the emissivity spectrum and temperature for a given pixel are presumably unknown as well, so there are more unknowns than available spectral channels. Atmospheric compensation and TES solutions have been developed using a variety of constraints on the spectrum and atmospheric representation as well as a variety of mathematical methods [1-5].

A straightforward hyperspectral TES approach suitable for materials with arbitrary emissivity was developed by Borel [6] based on maximizing emissivity spectral smoothness, and was later extended to atmospheric retrieval [7]. In this paper, we describe a related smoothness-based automated atmospheric compensation and TES method, called FLAASH-IR (Fast Line-of-sight Atmospheric Analysis of Spectral Hypercubes – InfraRed), and its application to imagery taken from an aircraft with the Telops Inc. Hyper-Cam interferometric hyperspectral imager. A recent paper [8] describes an application of FLAASH-IR to ground-to-ground Hyper-Cam imagery.

2. CALCULATION OVERVIEW

The LWIR spectral radiance measured by a sensor viewing objects on the ground can be written as

$$L_{obs}(\lambda) = B(T, \lambda)\varepsilon(\lambda)\tau(\lambda) + [1 - \varepsilon(\lambda)]L^{\downarrow}(\lambda) + L^{\uparrow}(\lambda) \qquad \textbf{(1)}$$

where λ is wavelength, $\varepsilon(\lambda)$ is the composition- and temperature-averaged spectral emissivity of the surface pixel, $\tau(\lambda)$ is the total (diffuse plus direct) transmittance between the surface and the sensor, $B(T, \lambda)$ is the surface Planck blackbody function at temperature T, $L^{\downarrow}(\lambda)$ is the transmitted incident illumination, and $L^{\uparrow}(\lambda)$ is the atmospheric path radiance. T is effectively an emissivity-weighted average within each pixel. Eq. (1) is rigorous for Lambertian surfaces; for specular surfaces the emissivity and illumination quantities may be regarded as "effective." In FLAASH-IR $\tau(\lambda)$, $L^{\downarrow}(\lambda)$ and $L^{\uparrow}(\lambda)$ are simulated for a given set of atmospheric properties using the MODTRAN5® model [9]. Hyperspectral channels are typically narrow

enough that within-channel variations in emissivity and the blackbody function can be neglected. Therefore the atmospheric radiance and transmittance parameters in Eq. (1) are convolved with the wavelength response functions and assigned to their center wavelengths.

2.1. Temperature and Emissivity Separation (TES)

For a given model atmosphere defining the transmittance, path and illumination radiances, Eq. (1) leads to a family of emissivity spectrum solutions corresponding to a range of possible surface temperature:

$$\varepsilon = (L - L^{\downarrow} - L^{\uparrow}) / (B(T)\tau - L^{\downarrow}) \quad \textbf{(2)}$$

The quantities in Eq. (2) are implicitly wavelength dependent. According to the smooth-emissivity criterion, the most likely solution is the one with the least spectral fine structure. A useful measure of emissivity fine structure is the mean square residual between the emissivity spectrum and the same spectrum smoothed with a running average over spectral channels, denoted as $<\varepsilon>$. A better measure, adopted in FLAASH-IR, is obtained by inserting $<\varepsilon>$ into Eq. (1) and taking the mean square of the difference between the computed radiance and the original data:

$$\sigma^2 = \underline{[L_{obs} - L(<\varepsilon>)]^2} \quad \textbf{(3)}$$

$$\text{where } L(<\varepsilon>) = B(T) <\varepsilon>\tau + (1 - <\varepsilon>)L^{\downarrow} + L^{\uparrow} \quad \textbf{(4)}$$

and the underline in Eq. (2) denotes the running average. The TES is performed by finding the minimum of σ^2. As this measure is uniformly weighted across all wavelengths, regardless of atmospheric optical depth, it enables inclusion of optically thick wavelengths, where emissivity is poorly determined but there is valuable information on the atmosphere. The unsmoothed emissivity spectrum from Eq. (2) is reported as the retrieval result. To reduce sensitivity to sensor artifacts, such as wavelength or instrument function miscalibration, we use a fairly wide smoothing window of around ~0.3-0.5 μm (typically ~7-11 channels), which suppresses coarse as well as fine spectral features.

The TES generally benefits from restricting the analysis to the ~9-10.2 μm region around the ozone band, whose presence in the surface spectrum directly correlates with reflectance (1-emissivity). However, for atmosphere retrieval the broad ~8-13 μm region is typically used, as its water vapor features are needed to characterize the water column density and lower atmospheric temperature.

2.2. Atmosphere and Emissivity Retrieval

The above σ^2 minimization approach is used to retrieve atmospheric parameters in addition to surface temperatures. We assume that the scene dimensions are small enough that a single, homogenous atmosphere suffices. The model calculations of $\tau(\lambda)$, $L^{\downarrow}(\lambda)$ and $L^{\uparrow}(\lambda)$ depend on assumed atmospheric species and temperature profiles. In the 8-13 μm region the most prominent atmospheric species is water vapor, and under clear conditions the key variables are the column water vapor and the air temperature near the ground.

The challenge is to specify a family of plausible and diverse trial atmospheres using a small number of variables. FLAASH-IR specifies a three-dimensional grid of parameters controlling surface air temperature, water vapor column density or humidity, and ozone concentration. The parameters, typically a temperature shift and concentration scalings, perturb the profiles of a user-selected seasonal/latitude MODTRAN model atmosphere. Tabulations of $\tau(\lambda)$, $L^{\uparrow}(\lambda)$ and $L^{\downarrow}(\lambda)$ spectra are derived from the MODTRAN5 outputs, and polynomial fitting is used to interpolate the spectra between these grid points. Partial cloud cover is modeled by blending the clear sky $L^{\downarrow}(\lambda)$ with a blackbody function.

The best-fit atmosphere model is retrieved from of order ten selected pixel spectra by minimizing the total σ^2 with respect to both T and the atmospheric parameters. The spectra are selected to be diverse in shape and brightness, so that different surface temperatures and emissivities are represented. Low emissivity (reflective) materials provide valuable information on $L^{\downarrow}(\lambda)$. The σ^2 minimization involves a one-dimensional surface temperature search on the selected pixels embedded within a three-dimensional atmosphere search, which is conducted using a downhill simplex method. Finally, the retrieved atmosphere is used in a one-dimensional search to derive surface temperature and emissivity or reflectance for each pixel in the image. The emissivity can be refined with a spectral "polishing" option [8], in which smoothed emissivity spectra retrieved from the selected pixels are input to a least squares procedure that recalculates some or all of the atmospheric components, $\tau(\lambda)$, $L^{\uparrow}(\lambda)$ and $L^{\downarrow}(\lambda)$, which are then used in subsequent retrievals.

3. EXPERIMENT

The Telops Inc. Hyper-Cam LW is a portable imaging Fourier transform infrared (FTIR) spectrometer operating in the 8-12 μm range. The detector is a 320x256 PV-MCT focal plane array detector that can be windowed and formatted to fit the desired image size and decrease the acquisition time. The pixel IFOV is 0.35 mrad, and spectral resolution is user selectable from 0.25 to 150 cm-1. The Hyper-Cam LW has recently been integrated into an aircraft for nadir-viewing measurements. The aircraft platform includes a motion-compensating mirror that stabilizes the images over acquisition times of typically ~1 s. Overlapping images can be acquired and assembled into georectified

mosaics. A visible camera is bore-sighted with the Hyper-Cam. The data analyzed here, at 6 cm-1 resolution, were taken of the Jean Gaulin refinery in Saint-Romuald, QC, Canada at 11:30 AM on May 6, 2013 from an altitude of 1.55 km. A 294x294-pixel sub-image of the mosaic is shown in Fig. 1a. The corresponding visible image is in Fig. 1b.

4. RESULTS

The refinery image was processed with FLAASH-IR using a base MODTRAN Subarctic Summer model atmosphere and a spectral polishing option. The diverse spectra for the atmosphere retrieval were taken as averages of pixel spectral clusters centered on automatically extracted endmembers. As surfaces become highly reflective, surface temperature becomes indeterminate; a lower bound of 7 C was assumed. The output image is in reflectance versus wavelength. The retrieved atmosphere has 1300 atm-cm of water vapor and a surface air temperature of 27 C. The latter is close to the recorded temperature of 25 C at the nearby Jean Lesage Airport.

Fig. 1c shows the retrieved sub-image reflectance in false color. Metal roofs, equipment coverings and pipes appear in bright contrast against the other materials. Fig. 1d shows the FLAASH-IR fit error, σ. Large errors, typically up to ~50 μflicks, appear at object edges. These large errors are caused by slight misregistrations of the frames in the interferogram, resulting in some spectral corruption. However, away from the edges the fit errors are much closer to those observed in static Hyper-Cam measurements [8], as low as ~6 μflicks in shadows, but several times larger than this with reflective surfaces. Fig. 1e shows the retrieved surface temperature map. The coolest shadows are around 17 C; the sunlit areas are up to ~50 C except for a few "hot spots", which may include sensor anomalies. The most reflective materials are pinned to the lower limit of 7 C.

Figs. 2a and b show example radiance and reflectance spectra of various materials in the image. Consistent with Fig. 1d, the reflectance "noise" is lowest for blackbodies near ambient temperature. The metallic radiance spectra are highly structured due to reflected downwelling illumination from the 9.6 μm ozone band and 8-9 μm water vapor lines; some residuals of these features appear in the reflectance spectra. Dirt areas, appearing in red, have quartz-like spectra typical of sandy soil. A green object in the radiance image has a V-shaped spectrum that we interpret as plate glass. Another spectrally distinct material is unknown.

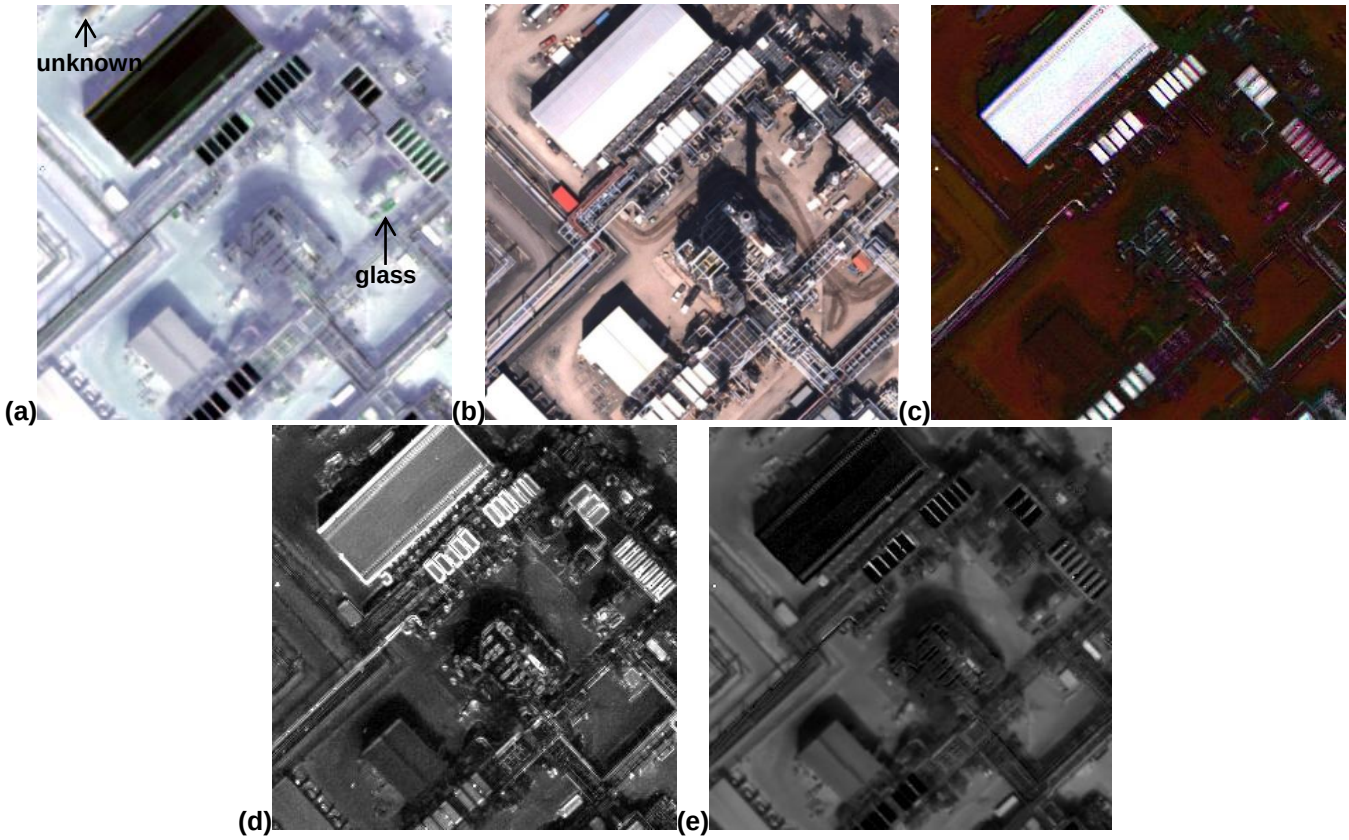

Fig. 1. (a) Original LWIR radiance image (RGB = 8.2, 9.7, 11.2 μm); (b) visible camera image; (c) retrieved LWIR reflectance image displayed as in (a); (d) error image; (e) surface temperature image (range=15-76 C).

A comparison of the unpolished and polished FLAASH-IR transmission spectra $\tau(\lambda)$ with the result from the In-Scene Atmospheric Compensation (ISAC) method of Young et al. [1] finds good agreement between the latter two. The path radiances $L^{\uparrow}(\lambda)$ show similar levels of agreement. However, as ISAC does not retrieve $L^{\downarrow}(\lambda)$ it cannot derive accurate spectra for reflective materials.

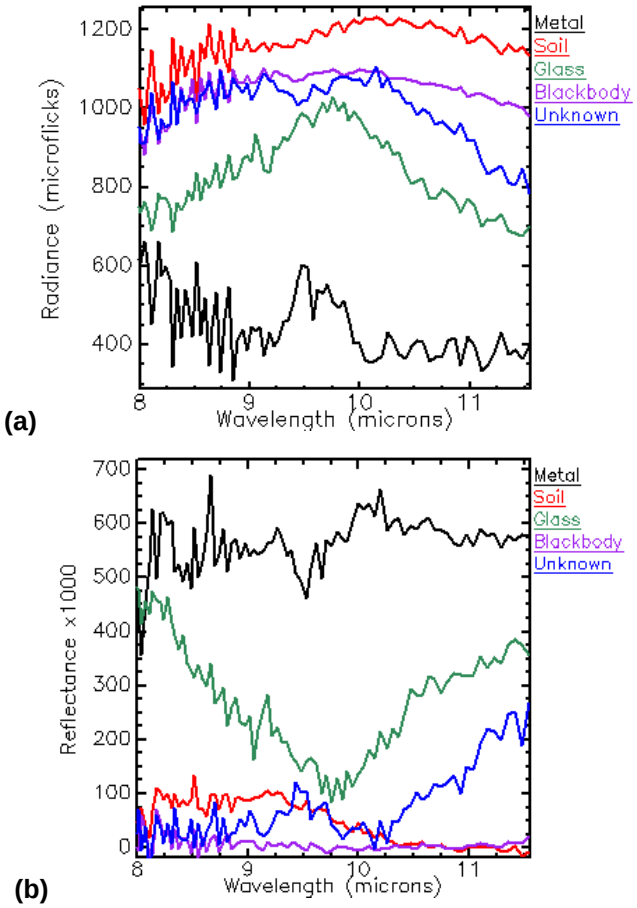

Fig. 2. Retrieved spectra from FLAASH-IR: (a) radiance, (b) reflectance.

5. SUMMARY AND CONCLUSIONS

Processing LWIR hyperspectral imagery to reflectance or emissivity via atmospheric compensation and TES affords the opportunity to classify and identify solid materials with minimal interference from the atmosphere. This is the first such study of data from an aircraft-mounted Hyper-Cam FTIR sensor. Acquiring FTIR imagery from a moving platform is extremely challenging due to the potential for both spatial misregistration and vibration effects on the optics. Not surprisingly, the reflectance results are noisier than what we have obtained from a stationary Hyper-Cam [8] as well as from some other sensors. The noise level might well be reduced with improvements in the hardware and software, but even with the present limitations the spectra and temperature maps should have considerable utility for remote object and material identification.

6. ACKNOWLEDGEMENTS

This work was supported by Spectral Sciences and Telops internal research and development. We thank Jeannette van den Bosch of the Air Force Research Laboratory for her valuable review of this manuscript.

7. REFERENCES

[1] S.J. Young, B.R. Johnson and J. A. Hackwell, "An In-scene Method for Atmospheric Compensation of Thermal Hyperspectral Data," *J. Geophys. Res. Atmospheres*, Vol. 204, pp. ACH 14-1 – ACH 14-20 (2002).

[2] D. Gu, A. R. Gillespie, A. B. Kahle, and F. D. Palluconi, "Autonomous Atmospheric Compensation of High Resolution Hyperspectral Thermal Infrared Remote-Sensing Imagery," *IEEE Trans. Geosci. Remote Sens.* 38, pp. 2557-2569 (2000).

[3] T. Matsunaga, "An Emissivity-Temperature Separation Technique Based on an Empirical Relationship Between Mean and Range of Spectral Emissivity," *Proc. 14th Japanese Conf. of Remote Sensing*, pp. 47-48 (1993).

[4] E.D. Hernandez-Baquero, and J. R. Schott, "Atmospheric compensation for surface temperature and emissivity separation," *SPIE Proceedings, Algorithms for Multispectral, Hyperspectral, and Ultraspectral Imagery VI*, Vol. 4049, pp. 400-410 (2000).

[5] M. Boonmee, J.R. Schott and D.W. Messinger, "Land surface temperature and emissivity retrieval from thermal infrared hyperspectral imagery," Algorithms and Technologies for Multispectral, Hyperspectral, and Ultraspectral Imagery XII, Sylvia Shen and Paul Lewis, eds., *Proc. SPIE* 6233, 62331V (2006).

[6] C.C. Borel, "Iterative Retrieval of Surface Emissivity and Temperature for a Hyperspectral Sensor," *First JPL Workshop on Remote Sensing of Land Surface Emissivity*, May 1997, pp. 1-5.

[7] C.C. Borel, , "ARTEMISS – an Algorithm to Retrieve Temperature and Emissivity from Hyper-Spectral Thermal Image Data," 28th Annual GOMACTech Conference, Hyperspectral Imaging Session, Tampa, FL, Los Alamos National Lab. Rpt. No. LA-UR-027907 (2003).

[8] S. Adler-Golden, P. Conforti, M.-A. Gagnon, P. Tremblay and M. Chamberland, "Long-wave Infrared Surface Reflectance Spectra Retrieved from Telops Hyper-Cam Imagery," *SPIE Proceedings, Algorithms for Multispectral, Hyperspectral and Ultraspectral Imagery*, in press (2014).

[9] A. Berk, , G.P. Anderson, P.K. Acharya, L.S. Bernstein, L. Muratov, J. Lee, M.J. Fox, S.M. Adler-Golden, J.H. Chetwynd, M.L. Hoke, R.B. Lockwood, T.W. Cooley and J.A. Gardner, "MODTRAN5: a Reformulated Atmospheric Band Model with Auxiliary Species and Practical Multiple Scattering Options," *Proc. SPIE Int. Soc. Opt. Eng*. 5655, 88 (2005).